

## Research Paper

# Time-Dependence of Molecular Mobility during Structural Relaxation and its Impact on Organic Amorphous Solids: An Investigation Based on a Calorimetric Approach

Chen Mao,<sup>1</sup> Sai Prasanth Chamrthy,<sup>1</sup> and Rodolfo Pinal<sup>1,2</sup>

Received December 9, 2005; accepted March 13, 2006

**Purpose.** To develop a calorimetry-based model for estimating the time-dependence of molecular mobility during the isothermal relaxation of amorphous organic compounds below their glass transition temperature ( $T_g$ ).

**Methods.** The time-dependent enthalpy relaxation times of amorphous sorbitol, indomethacin, trehalose and sucrose were estimated based on the nonlinear Adam-Gibbs equation. Fragility was determined from the scanning rate dependence of  $T_g$ . Time evolution of the fictive temperature was determined from  $T_g$ , the heat capacity of the amorphous and crystalline forms, and from the enthalpy relaxation data.

**Results.** Relaxation time changes significantly upon annealing for all compounds studied. The magnitude of the increase in relaxation time does not depend on any one parameter but on four parameters:  $T_g$ , fragility, and the crystal-liquid and glass-liquid heat capacity differences. The obtained mobility data for indomethacin and sucrose, both stored at  $T_g - 16$  K, correlated much better with their different crystallization tendencies than did the Kohlrausch-Williams-Watts (KWW) equation.

**Conclusions.** The observed changes in relaxation time help explain and address the limitations of the KWW approach. Due consideration of the time-dependence of molecular mobility upon storage is a key element for improving the understanding necessary for stabilizing amorphous formulations.

**KEY WORDS:** amorphous; fictive temperature; glass transition; molecular mobility; relaxation.

## INTRODUCTION

An important step toward the successful development of delivery systems of drugs in the amorphous state is the kinetic stabilization of amorphous pharmaceutical materials below their glass transition temperature ( $T_g$ ). The enhanced molecular mobility of amorphous compounds, relative to their crystalline form, is thought to be the cause of their significant tendency toward crystallization (1,2), chemical degradation (3,4), and structural collapse (5). A quantitative assessment of molecular mobility is, therefore, of critical importance for determining suitable storage conditions for amorphous compounds and their formulations. The molecular mobility of amorphous materials, usually expressed as the relaxation time,  $\tau$ , is typically evaluated through rate measurements of certain relaxation processes. From a stability perspective, storage conditions under which the materials exhibit relaxation times comparable to, or greater than the timescale of the shelf life are desirable.

Different techniques have been applied to study relaxation phenomena in amorphous pharmaceutical systems.

These include differential scanning calorimetry (DSC) (6,7), isothermal microcalorimetry (8,9), dielectric analysis (10,11), mechanical analysis (12,13), and solid-state NMR spectroscopy (14,15). Among them, the most frequently employed approach for estimating molecular mobility in amorphous solids is that of enthalpy recovery experiments using DSC. In these experiments, the amorphous solid is allowed to relax, for certain length of time, at a temperature below  $T_g$  (annealing). The enthalpy lost during annealing,  $\Delta H_{relax}$ , is recovered upon heating of the sample to a temperature above  $T_g$ , and can be measured by DSC. An average relaxation time  $\tau$ , and the stretched-time function parameter,  $\beta$ , can then be then obtained by fitting the enthalpy data to the empirical Kohlrausch-Williams-Watts (KWW) equation:

$$\phi = 1 - \frac{\Delta H_{relax}}{\Delta H_{\infty}} = \exp \left[ -\left(\frac{t}{\tau}\right)^{\beta} \right] \quad (1)$$

where  $\Delta H_{\infty}$  represents the total enthalpy available for relaxation before the glass reaches the equilibrium supercooled liquid state, and  $\phi$  is often called the relaxation function. Although widely accepted as the routine way of estimating molecular mobility, the underlying assumptions of this method present some limitations to its ability to describe the true relaxation behavior (7,16). One assumption in Eq. (1) is that the structural relaxation time  $\tau$  is constant throughout

<sup>1</sup> Department of Industrial and Physical Pharmacy, Purdue University, 575 Stadium Mall Drive, West Lafayette, Indiana 47907, USA.

<sup>2</sup> To whom correspondence should be addressed. (e-mail: rpinal@purdue.edu)

the relaxation process. In reality,  $\tau$  tends to increase as relaxation of the glass progresses. It follows that if the change in  $\tau$  during relaxation is sufficiently pronounced, it will lead to a situation where no single  $\tau$  value is sufficient to properly describe the relaxation process. This important point has been recently brought forth by Kawakami and Pikal (6) from the results of numerical simulations using the KWW kinetic model. They reported that changes in  $\tau$  of one to two orders of magnitude were possible over a period of 100 h of relaxation at reasonable temperatures below  $T_g$ . To the best of our knowledge, no experimental method has been reported for quantifying the change in relaxation time that accompanies structural relaxation.

The aim of this study is to develop a method for quantifying the time-dependence of molecular mobility using DSC, and to investigate the factors that contribute to the dynamics of molecular mobility during annealing. In this report, we present experimental results showing that the dynamics of change of molecular mobility during relaxation is significant enough as to make (standard) KWW-based enthalpy recovery methods inapplicable in many cases. Our results also show that the time evolution of  $\tau$  can help explain why amorphous compounds with similar  $T_g$  can exhibit substantially different crystallization tendencies under the same conditions. Awareness and estimation of a time-dependent molecular mobility merit attention for explaining or predicting stability-related issues of amorphous pharmaceuticals.

## METHOD DEVELOPMENT

The time-dependent structural relaxation times of organic glass materials were evaluated within the framework of the Adam-Gibbs theory (17). The original Adam-Gibbs (AG) equation describes a glass state relaxation controlled by configurational entropy:

$$\tau = \tau_0 \exp\left(\frac{\Delta\mu s_c^*}{k_B T S_c(T)}\right) \quad (2)$$

where  $\tau$  represents the relaxation time below the glass transition temperature,  $\tau_0$  is the pre-exponential factor,  $T$  is the absolute temperature,  $S_c(T)$  is the configurational entropy at temperature  $T$  and  $k_B$  is Boltzmann's constant. The terms  $s_c^*$  and  $\Delta\mu$  denote the entropy of the smallest cooperative molecular region and the activation energy of cooperative rearrangement, respectively, and are properties of the glass-forming liquid.

Equation (2) implies that for an isothermal relaxation process, changes in the relaxation time are entirely determined by changes in the configurational entropy,  $S_c(T)$ . This means that if  $S_c(T)$  remains unchanged upon storage of the amorphous material,  $\tau$  becomes a time-independent parameter. However, as a glassy material relaxes toward a denser structure, its configurational entropy is bound to decrease due to the accompanying reduction in configurational degrees of freedom. Consequently,  $\tau$  tends to increase as the relaxation progresses. This study is intended to evaluate the magnitude of such changes following an isothermal structural relaxation process.

The time-dependence of  $S_c(T)$  can be conveniently expressed through the fictive temperature,  $T_f$ , originally introduced by Tool (18). The fictive temperature is defined as the thermodynamic temperature at which some observed non-equilibrium property, *in excess to the stable crystalline form*, would be the equilibrium value (See Fig. 1). From these considerations,  $S_c(T, t)$  of a glass becomes  $S_c(T_f)$ . It is readily seen from Fig. 1 that the loss of the configurational entropy during structural relaxation corresponds to a lowering of  $T_f$ , so that  $S_c(T_f)$  becomes a time-dependent value and can be calculated from:

$$S_c(T_f) = \int_{T_2}^{T_f} \frac{\Delta C_p'(T)}{T} dT \quad (3)$$

where  $\Delta C_p'(T)$  is the heat capacity difference between the liquid and crystalline phases (19) and  $T_2$  is the temperature at which the configurational entropy falls to zero (20), which by definition is identical to the thermodynamic Kauzmann temperature  $T_K$  (19). The quantity  $S_c(T_f)$  can be evaluated if the temperature dependence of  $\Delta C_p'$  is known. The most frequently used relationship is the hyperbolic expression:

$$\Delta C_p'(T) = \frac{\Delta C_p'(T_2) T_2}{T} \quad (4)$$

Combining Eqs. (2), (3) and (4) results in the well known nonlinear AG equation:

$$\tau = \tau_0 \exp\left(\frac{B}{T(1 - T_2/T_f)}\right) \quad (5)$$

$$B = \frac{\Delta\mu s_c^*}{k_B \Delta C_p'(T_2)} \quad (6)$$

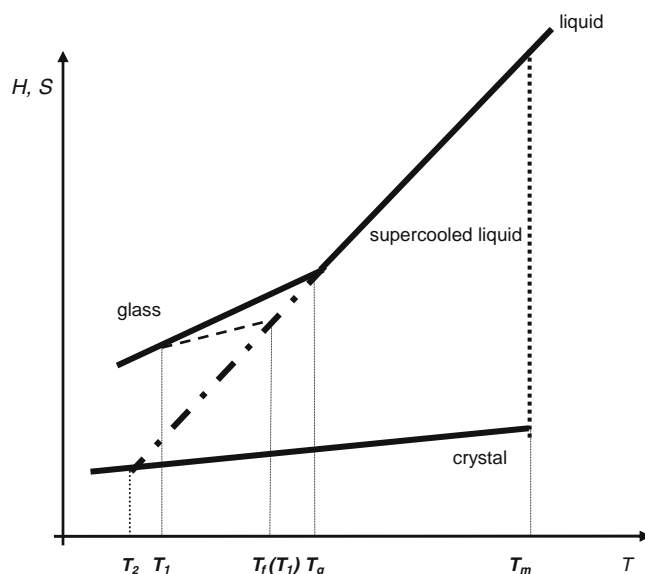


**Fig. 1.** Schematic diagram describing the fictive temperature  $T_f$  of the amorphous state.

Equation (5) is frequently applied to describe nonlinear relaxation of both polymeric and non-polymeric materials below their  $T_g$ . When the temperature is at or above  $T_g$ , the material re-assumes equilibrium liquid state, namely  $T_f = T$ , and Eq. (5) reduces to the Vogel-Tammann-Fulcher (VTF) equation:

$$\tau = \tau_0 \exp\left(\frac{B}{T - T_0}\right) \quad (7)$$

where the zero configurational entropy temperature  $T_2$  in Eq. (5) is numerically equivalent to  $T_0$  in Eq. (7). It is worthwhile to mention that while the nonlinear AG equation was derived from statistical thermodynamic considerations, the VTF equation was obtained empirically from the observed behavior of liquids, specifically, from the (non-Arrhenius) dependence of viscosity on temperature as  $T_g$  is approached. The connection between Eqs. (5) and (7) carries an important notion. Namely, that the parameters  $B$  and  $T_2$  in Eq. (5), which describe structural relaxation below  $T_g$ , are also characteristic of the liquid, and can therefore be evaluated entirely from the liquid state above  $T_g$  from the VTF equation (Eq. 7). Such a strategy has been used for estimating activation energy of the glass state by fitting the VTF equation in liquid state (21).

We chose the nonlinear AG equation (Eq. 5) to evaluate the time-dependence of relaxation time in this study. For convenience, we make a notation change by replacing  $T_2$  with  $T_0$  in Eq. (5), so that our working equation becomes:

$$\tau = \tau_0 \exp\left(\frac{B}{T(1 - T_0/T_f)}\right) \quad (8)$$

Equation (8) is numerically indistinguishable from Eq. (5), so that the time dependence of  $\tau$  is completely determined by the changes in  $T_f$ . The practical significance of this approach is that the changes in question can be measured using DSC. The following section focuses on the calorimetric assessment of the parameters in Eq. (8) ( $B$ ,  $T_0$  and  $T_f$ ) in order to estimate the time-dependent relaxation times of organic compounds in the glassy state.

### Evaluation of $B$ and $T_0$

The VTF equation can be re-written as the temperature-dependence of the apparent activation enthalpy,  $\Delta H^*$ :

$$\frac{\Delta H^*}{R} = \frac{d \ln \tau}{d(1/T)} = \frac{B}{(1 - T_0/T)^2} \quad (9)$$

where  $R$  is the gas constant. It is clear from the equation above that if values of  $B$  and  $T_0$  are known, one can calculate the apparent activation enthalpy of relaxation for the liquid at any temperature  $T$ , provided that  $T \geq T_g$ . Moynihan *et al.*

(22,23) showed that the activation enthalpy at  $T_g$  can be estimated from the heating/cooling rate (denoted by  $q$ ) dependence of  $T_g$ :

$$\frac{\Delta H^*(T_g)}{R} = - \frac{d \ln q}{d(1/T_g)} \quad (10)$$

The apparent activation enthalpy at  $T_g$ ,  $\Delta H^*(T_g)$ , can be determined using DSC by heating or cooling the amorphous materials at different rates and plotting  $\ln q$  vs. the obtained  $1/T_g$ . Such an approach, although originally developed for and tested on inorganic materials, has been successfully applied to the study of organic pharmaceutical compounds (3,11,24). The value of  $\Delta H^*(T_g)$  alone, however, is not sufficient to solve for both  $B$  and  $T_0$  in Eq. (9). In order to address this point, we make use of the fragility parameter,  $m$ , defined as the apparent activation enthalpy scaled by the available thermal energy at  $T_g$  (25,26):

$$m = \left. \frac{d \log \tau}{d(T_g/T)} \right|_{T=T_g} = \frac{\Delta H^*(T_g)}{(\ln 10)RT_g} \quad (11)$$

The value of  $m$  can be experimentally determined from Eq. (10). Substituting Eq. (11) into Eq. (9) yields the relationship between  $m$ ,  $B$  and  $T_0$ :

$$m = \frac{B/T_g}{(\ln 10)(1 - T_0/T_g)^2} \quad (12)$$

Even though Eq. (12) has still the same two unknowns ( $B$  and  $T_0$ ) as Eq. (9), the transformation allow us to take advantage of some general properties of glasses, as will be detailed below.

The minimum possible fragility value,  $m_{min}$ , corresponds to the relaxation of the unrestricted material at  $T_g$ , such that Arrhenius behavior applies. Therefore,  $m_{min}$  will be given as:

$$m_{min} = \frac{\Delta H_{min}^*}{(\ln 10)RT_g} = \log\left(\frac{\tau(T_g)}{\tau_0}\right) \quad (13)$$

where  $\Delta H_{min}^*$  corresponds to the activation enthalpy Eq. (10) for a material that conforms exactly to the Arrhenius behavior, in other words, a material that exhibits the minimum possible fragility. Notice that this idealized condition makes the relationship between  $\Delta H_{min}^*$  and  $T_g$  such, that if one is known the other one is fixed. The relaxation time at  $T_g$ ,  $\tau(T_g)$ , is in general in the order of 100 s for both organic and inorganic materials (26,27). The minimum relaxation time,  $\tau_0$ , on the other hand, can be approximated as the timescale of atomic vibrations at  $10^{-14}$  s. From these considerations, we arrive to  $m_{min} = 16$  as being applicable to glasses in general. Combining the VTF equation Eqs. (7) and (13) for the temperature  $T = T_g$  gives:

$$m_{min} = \frac{B}{\ln(10)(T_g - T_0)} \quad (14)$$

From the known values for  $m$  [Eq. (11)] and  $m_{\min}$ , the values for  $B$  and  $T_0$  can be obtained from Eqs. (12) and (14) as follows:

$$T_0 = T_g \left( 1 - \frac{m_{\min}}{m} \right) \quad (15)$$

$$B = \frac{(\ln 10) T_g m_{\min}^2}{m} \quad (16)$$

Equations (15) and (16) show that the parameters needed to evaluate  $B$  and  $T_0$  can all be experimentally obtained from DSC measurements based on the heating/cooling rate dependence of  $T_g$ . This method is experimentally more favorable than the traditional way of fitting the VTF equation since it does not require to maintain the sample above  $T_g$  for prolonged periods during the measurements. Pharmaceutical organic compounds in the supercooled liquid state often exhibit chemical and physical instability during calorimetric measurement of molecular mobility above  $T_g$  (24).

### Evaluation of the Fictive Temperature

Equation (2) defines the fictive temperature in terms of configurational entropy. In an analogous manner, the fictive temperature can be expressed in terms of enthalpy, namely:

$$H_c(T_f) = \int_{T_2}^{T_f} \Delta C_p'(T) dT \quad (17)$$

where  $H_c(T_f)$  denotes the configurational enthalpy of the glass. Consider the relaxation of a glassy material after

cooling it below  $T_g$  to a temperature  $T_1$ . The initial fictive temperature,  $T_f^0$ , should be determined in order to calculate the initial configurational enthalpy available at the onset of the relaxation process. For simplicity, the common practice is to approximate  $T_f^0$  as being equal to  $T_g$  (11,28). This assumption, however, is valid only when the annealing temperature  $T_1$  is very close to  $T_g$  or when the heat capacities of the glass and crystalline forms are very close to each other. In reality, cooling the glass from  $T_g$  to  $T_1$  involves a loss of configurational enthalpy, making  $T_f^0$  smaller than  $T_g$  as seen in Fig. 2. In the figure, the dotted line connecting the enthalpy of the fresh glass with the enthalpy of the liquid (at  $T_f^0$ ) is parallel to the line of the crystal form. Only when the heat capacity of the glass and the crystal are the same, the two corresponding lines in the figure should be parallel, making  $T_f^0 = T_g$ . However, since the line of the glass is always steeper (higher heat capacity) than that of the crystal (as well as the dotted) line, cooling below  $T_g$  always results in  $T_f^0 < T_g$ .

The excess enthalpy,  $\Delta H_\infty(T_1)$ , can be expressed in two alternative ways, either in terms of  $T_g$  or in terms of  $T_f^0$  (See Fig. 2):

$$\Delta H_\infty(T_1) = \int_{T_1}^{T_g} \Delta C_p(T) dT = \int_{T_1}^{T_f^0} \Delta C_p'(T) dT \quad (18)$$

where  $\Delta C_p$  is heat capacity difference *between the liquid and glass forms*.  $\Delta C_p'$ , as defined earlier, is the heat capacity difference *between the liquid and crystalline forms*. If the temperature dependence of the heat capacity terms in Eq. (18) is known, the value of  $T_f^0$  can be obtained. Assuming (again) a hyperbolic temperature dependence of heat capacity we obtain:

$$T_f^0 = T_g^\gamma \cdot T_1^{(1-\gamma)} \quad (19)$$

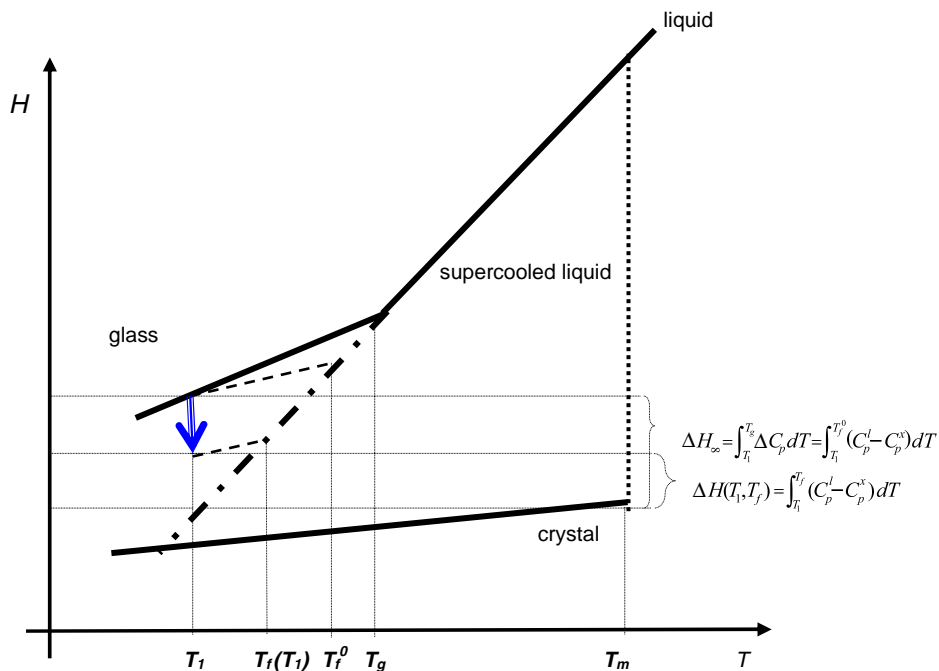


Fig. 2. Schematic diagram of enthalpic relaxation. The loss of enthalpy during relaxation can be expressed with enthalpic fictive temperature.

$$\gamma = \frac{\Delta C_p}{\Delta C_p'} \Big|_{T_g} \quad (20)$$

The parameter  $\gamma$ , originally proposed by Shamblin *et al.* (29), ranges between 0 and 1, with  $\gamma = 1$  corresponding to equivalent heat capacities for the glass and crystal forms at  $T_g$ . The value of  $T_f^0$  provides information about the configurational enthalpy available in the fresh (un-annealed) glass at  $T_1$ . It is important to point out that  $T_f^0$  discussed here is enthalpic in origin. The entropic  $T_f^0$  can be obtained following a similar derivation (29). The relaxation time of a fresh glass  $\tau_{glass}^0$  can be obtained by substituting Eq. (19) into Eq. (8):

$$\tau_{glass}^0 = \tau_0 \exp\left(\frac{B}{T_1 - T_0(T_1/T_g)^\gamma}\right) \quad (21)$$

Since the annealing temperature  $T_1$  is lower than  $T_g$ , a greater value of  $\gamma$  corresponds to a less pronounced temperature dependence of molecular mobility in the fresh glass. In the limit  $\gamma = 1$ , the glass follows Arrhenius behavior. In the other limit, i.e., when  $\gamma = 0$ , Eq. (21) reduces to the VTF equation, describing the equilibrium behavior of the liquid.

The time-dependence of molecular mobility is reflected by changes in  $T_f$ . As the relaxation proceeds, the enthalpy of the glass decreases. The instantaneous excess enthalpy during the relaxation depends on  $T_f$  and is given by (Fig. 2):

$$\Delta H(T_1, T_f) = \int_{T_1}^{T_f} \Delta C_p' dT = \int_{T_1}^{T_f} \frac{\Delta C_p}{\gamma} dT \quad (22)$$

The fraction of enthalpy relaxed,  $\Delta H_{relax}$ , during the experiment is the difference between the initial and the instantaneous excess enthalpy available and can be expressed by subtracting Eq. (22) from Eq. (18):

$$\Delta H_{relax} = \int_{T_f}^{T_g} \frac{\Delta C_p}{\gamma} dT \quad (23)$$

This amount of enthalpy, lost during relaxation, is recovered by heating the sample through  $T_g$  and can be readily measured from the endothermic peak associated with the glass transition event during DSC determinations (10,12,30). Recalling the previously made assumption [Eqs. (4) and (19)] of a hyperbolic temperature dependence of  $\Delta C_p$ , the fictive temperature  $T_f$  can be obtained from Eq. (23) as:

$$T_f = T_f^0 \exp\left(-\frac{\gamma \Delta H_{relax}}{\Delta C_p T_g}\right) \quad (24)$$

Form Eq. (24), the experimental determination of  $T_f$  becomes a simple calculation because it only requires the value of  $\Delta C_p$  at  $T_g$ . Calorimetric measurements of  $\Delta C_p T_g$  are now routine practice in the evaluation of the initial excess enthalpy of amorphous pharmaceutical compounds (6). This is so even though it has been reported that due to possible

contributions from vibrational degrees of freedom,  $\Delta C_p T_g$  may in reality be an overestimate of configurational heat capacity (31).

It is important to point out that the fictive temperature  $T_f$  in our working equation Eq. (8) is an entropy-based value, whereas the fictive temperature in Eqs. (17) through (24) is of enthalpic origin. The reason for changing from one to the other is entirely a practical one: whereas direct and accurate enthalpy measurements are readily obtainable with DSC, non-equilibrium entropy determinations are no simple task. The assumption here is that the enthalpy- and entropy-based fictive temperatures are the same. In other words, that the degree of relaxation of the sample is the same, whether we are looking at it from an enthalpy or from an entropy point of view. With this assumption, Eqs. (8) and (21) are equivalent expressions.

The above discussion leads to the development of the experimental procedure for the evaluation of the time-dependent relaxation time,  $\tau$ , on the basis of the Adam-Gibbs formulation for nonlinear relaxations. Eq. (8) will be used as our working equation. The experimental procedure is as follows:

1. Evaluating  $B$  and  $T_0$  from scanning rate dependence of  $T_g$  using DSC Eqs. (9) through (16).
2. Measuring of  $\Delta C_p T_g$  and  $\gamma$  by DSC Eq. (20).
3. Calculating the initial enthalpic fictive temperature  $T_f^0$  from  $T_g$  and  $\gamma$  Eq. (19).
4. Evaluating time-dependent  $T_f$  by measuring recovered enthalpy using DSC after allowing samples to relax for given lengths of time Eq. (24).
5. Calculating the time-dependent relaxation time,  $\tau$  Eq. (8).

## MATERIALS AND METHODS

### Materials

Indomethacin and sorbitol, both of highest grade available, were purchased from Sigma (St. Louis, MO). Amorphous indomethacin and sorbitol were prepared in the DSC by heating the samples above their melting points followed by cooling the melt at the rate of  $20 \text{ K}\cdot\text{min}^{-1}$ . The lack of crystallinity was confirmed by the complete absence of melting endotherm at their corresponding melting temperatures.

### Differential Scanning Calorimetry (DSC)

A 2920 model DSC (TA Instruments, New Castle, DE) with modulated DSC (MDSC) capability, attached to a refrigerated cooling accessory was used in this study. The standard (conventional) DSC mode was adopted for  $T_g$  measurements and enthalpy relaxation endotherms. The temperature-modulation mode was used to measure the differences in heat capacity between different forms at  $T_g$ . Samples (5–10 mg) were loaded into aluminum pans and analyzed with closed pan configuration under dry nitrogen purge. The cell constant and temperature calibrations were conducted using indium standard.

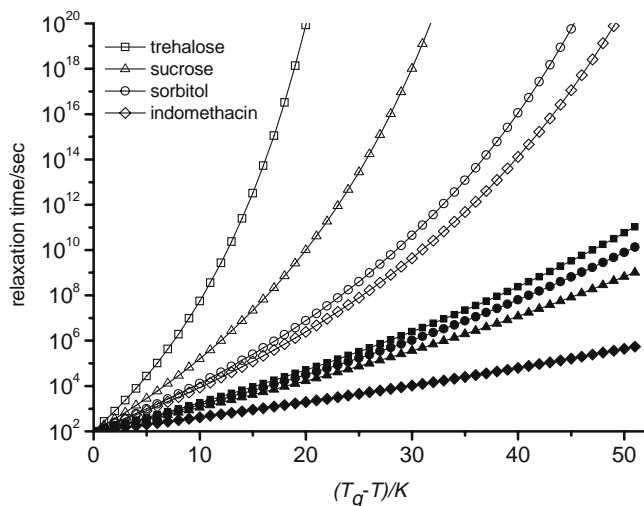


**Fig. 3.** Estimated relaxation times for liquids (Eq. (7), open symbols) and fresh glasses (Eq. (21), solid symbols) of selected pharmaceutical compounds as the function of  $T_g - T$ .

### Heat Capacity Measurements

The heat capacity of crystalline and amorphous materials was determined using MDSC. The cell constant and temperature calibration were conducted using indium standard at a nominal heating rate of  $2 \text{ K}\cdot\text{min}^{-1}$ . The heat capacity calibration constant ( $K_{Cp}$ ) was obtained by running a sapphire disc under a nominal heating rate of  $2 \text{ K}\cdot\text{min}^{-1}$ , period of 100 s and amplitude of 0.5 K in the same pan as the sample. An independent calibration was performed for each replicate. Each sample was measured in triplicate. The heat capacities of samples were obtained from the data analysis software available with the instrument. The heat capacity values were measured in a range from 20–50 K below  $T_g$  to about 20 K above  $T_g$ .

### Enthalpy Recovery Experiments

The enthalpy loss during isothermal relaxation was measured using the method originally proposed by Hancock *et al.* (12). Amorphous samples were heated to 10 K above  $T_g$ , followed by cooling to 50 K below  $T_g$  in order to remove any thermal history. The samples were then heated to the desired temperature and held, isothermally, for 0.5, 1, 2, 4, 8, and 16 h before they were cooled to 50 K below  $T_g$  and then heated to 10 K above  $T_g$ , all at the rate of  $10 \text{ K}\cdot\text{min}^{-1}$ . The enthalpy lost during relaxation was measured from the endotherm associated with the glass transition. Data used in the study were averaged from three independent runs at each temperature for each material.

### Scanning Rate Dependence of $T_g$

The scanning rate dependence of  $T_g$  was obtained using the method proposed by Moynihan *et al.* (23). Experiments were performed at five different heating rates ( $0.5, 2, 5, 10$  and  $20 \text{ K}\cdot\text{min}^{-1}$ ). The  $T_g$  was measured during the second scan after a first scan to 10 K above  $T_g$  and a subsequent cooling to 50 K below  $T_g$  at the same rate. The mid-point temperature was obtained from three independent DSC runs.

## RESULTS

### Thermodynamic Potential for Changes in Molecular Mobility during Relaxation

For an amorphous pharmaceutical compound in the glassy state undergoing isothermal structural relaxation, the supercooled liquid is generally regarded as the immediate thermodynamic equilibrium state toward which the glass relaxes. The lowest molecular mobility the glass can attain is that of the supercooled liquid at the same temperature. Comparing the relaxation time of the supercooled liquid with that of the fresh (un-annealed) glass would make it possible to obtain information about the dynamics of molecular mobility during relaxation.

The relaxation times of indomethacin, sorbitol, trehalose and sucrose below  $T_g$ , both as liquids and as freshly prepared glasses, are shown in Fig. 3 as functions of  $T_g - T$ . The  $\tau$  values of the liquids and the glasses were calculated from Eqs. (7) and (21), respectively. Figure 3 shows that for all compounds investigated, the relaxation times of the liquids and glasses quickly diverge when the temperature falls below  $T_g$ . The figure also shows that the rank order in  $\tau$  values above and below  $T_g$  are not the same. At 20 K below  $T_g$ , the  $\tau$  ratios of liquids versus fresh glasses range from 250 (sorbitol) to  $2 \times 10^{17}$  (trehalose). These differences, which can be dramatic, provide sufficient thermodynamic potential for molecular mobility changes during relaxation.

The difference in  $\tau$  between liquids and fresh glasses can also be obtained by taking the ratio of Eqs. (7) and (21) as:

$$\frac{\tau_{\text{liquid}}}{\tau_{\text{glass}}^0} = \exp \left[ B \left( \frac{1}{T - T_0} - \frac{1}{T - T_0 (T/T_g)^\gamma} \right) \right] \quad (25)$$

where  $\tau_{\text{glass}}^0$  represents the relaxation time of the fresh glass. Eq. (25) shows that the divergence between the molecular mobility of glasses and liquids not only depends on  $T_g$  and fragility ( $m$ ), but it is also influenced by the  $\gamma$  term, which

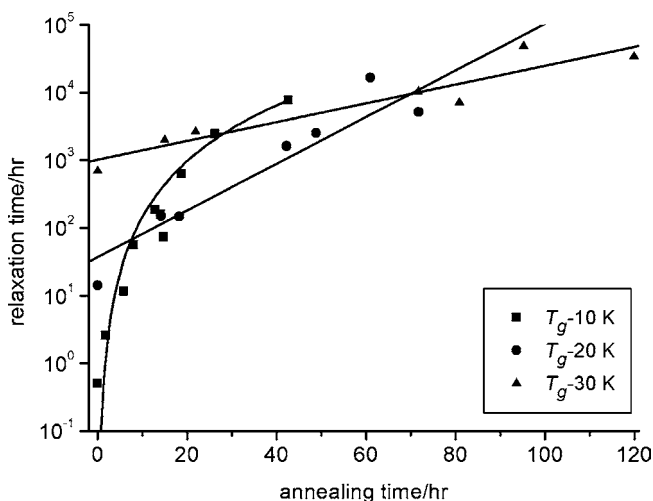


**Fig. 4.** Changes in  $\tau$  with time for amorphous trehalose annealed at different temperatures below  $T_g$ . The plotted points were obtained from the experimental  $\Delta H_{\text{relax}}$  values and Eqs. (8) and (24). The lines are shown as visual aid.

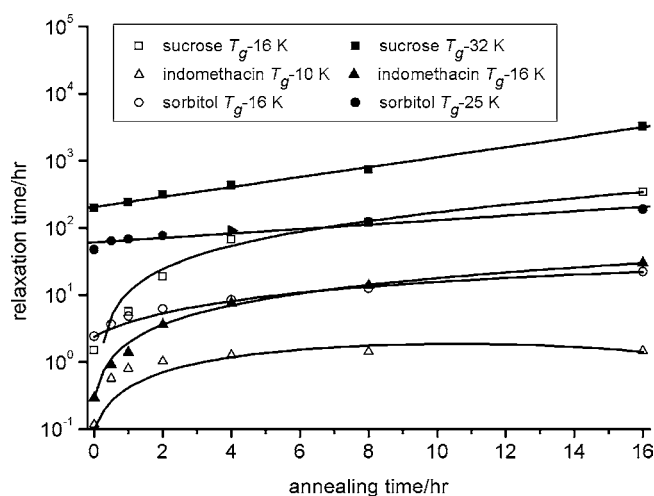


**Fig. 5.** Changes in relaxation time with time for amorphous sucrose, indomethacin and sorbitol annealed at different temperatures below  $T_g$ . The plotted points were obtained from the experimental  $\Delta H_{\text{relax}}$  values and Eqs. (8) and (24). Lines are shown as visual aid.

involves the heat capacities of the crystalline, glassy and liquid states. Eq. (25) shows that the greater the heat capacity difference between the crystal and glass forms, the greater the potential for changes in molecular mobility during relaxation.

#### Changes in Molecular Mobility during Relaxation

The  $\tau$  values for trehalose, sorbitol, indomethacin and sucrose as a function of annealing time at different temperatures are shown in Figs. 4 and 5. The relaxation times were obtained from the enthalpy recovery data and the methods summarized in the Method Development section. The parameters needed to calculate the relaxation times were measured using DSC and MDSC and are listed in Table I.

Significant increases in  $\tau$  are evident from Figs. 4 and 5 for all four compounds at all temperatures investigated. Within 16 h of annealing, the estimated increases in relaxation times varied from a factor of 4 (sorbitol at  $T_g-25$  K) to a factor of 225 (sucrose at  $T_g-16$  K). For relaxation over longer periods of time, changes in the estimated  $\tau$  by four orders of magnitude were observed. In a recent article, Kawakami and Pikal (6) investigated the changes in relaxation time of two types of amorphous organic

compounds through a theoretical simulation. The simulation was performed by breaking the continuous annealing process into many individual short time intervals. The relaxation of each small time section was characterized by the KWW equation (with an estimated  $\beta$  value), with its corresponding  $\tau$  value obtained from the nonlinear AG equation using the  $T_f$  of the preceding time step. Our experimental results show agreement with the results from those simulations, i.e., significant changes in molecular mobility can and do occur during the timescale of the annealing experiment. Our calculations suggest that the changes in relaxation time taking place during annealing can be even greater than previously anticipated. Changes in molecular mobility during relaxation can lead to changes in  $\tau$  that span several orders of magnitude within the experimental timescale. In such cases, no single  $\tau$  value can possibly provide sufficient information for a full account of the relaxation behavior over the timescale of the experiment. This means that changes in molecular mobility during relaxation can be of such magnitude as to render the concept of *mean* relaxation time inadequate to properly describe the molecular motions of some glassy state pharmaceuticals. It is therefore reasonable to question the reliability of the estimated mean relaxation times obtained by fitting the KWW equation, since these estimates are made by assuming a constant relaxation time during the enthalpy recovery experiments. Further discussion on the adequacy of the KWW equation is provided in the following section.

The obtained results show that changes in molecular mobility are strongly affected by the initial relaxation time, which rapidly increases as the annealing temperature moves away from  $T_g$  (see Fig. 3). For a given compound, a longer  $\tau$  at the onset of the relaxation process typically leads to slower evolution of molecular mobility during the relaxation that follows. Therefore, the reason for storing amorphous materials at temperatures significantly below  $T_g$  can be considered two-fold: a) to reduce the molecular motion, but also, b) to suppress the time dynamics (curvature) of molecular mobility so that the stability of the material can be more easily predicted. Our results show that changes in  $\tau$  with time cannot be fitted to any particular type of function. Although it is modeled by an exponential function [Eq. (8)], the  $\tau$  values are dependent on changes in the fictive temperature  $T_f$ , which does not maintain a linear relationship with time, and can only be estimated from enthalpy recovery experiments. In fact, the nonlinear and nonexponential nature of structural relaxation are both reflected on the dynamics of  $T_f$ .

**Table I.** The Calorimetrically Determined Values of  $T_g$ ,  $m$ ,  $B$ ,  $T_0$ ,  $\Delta C_{p,T_g}$  and  $\gamma$  for the Selected Amorphous Compounds

	$T_g$ (K)	$m$	$B$	$T_0$ (K)	$\Delta C_{p,T_g}$ ( $\text{J}\cdot\text{g}^{-1}\cdot\text{K}^{-1}$ )	$\gamma^c$
Sorbitol	271.75	50.8	3,152.7	186.19	0.80	0.61
Indomethacin	317.65	54.7	3,421.5	224.79	0.42	0.92
Trehalose <sup>a</sup>	390.35	165	1,394.8	352.50	0.55	0.80
Sucrose <sup>b</sup>	350	93.3	2,210.9	290	0.56	0.76

<sup>a</sup>  $T_g$ ,  $m$ , and  $\Delta C_{p,T_g}$ , data from (42);

<sup>b</sup>  $T_g$ ,  $T_0$ , and  $\Delta C_{p,T_g}$  data were from (29).

<sup>c</sup> All  $\gamma$  values from (29).

## DISCUSSION

## Factors Controlling Changes in Molecular Mobility

In order to better understand the dynamics of molecular mobility, it is critical to investigate the material properties controlling the rate of change in relaxation time. The contributing properties can be identified from the nonlinear AG equation [Eq. (8)] used in this study. Among all parameters in Eq. (8), the only time-dependent value is the fictive temperature  $T_f$ , which was obtained from the time-dependence of the relaxation enthalpy  $\Delta H_{\text{relax}}$  during annealing. Unfortunately, to date there is no mechanistic model generally accepted for  $\Delta H_{\text{relax}}$ , except for the empirical KWW equation, which relates  $\Delta H_{\text{relax}}$  to  $\tau$ . However, incorporation of the KWW equation into the nonlinear AG equation in order to predict the time evolution of  $\tau$  is not feasible because of the unknown stretch parameter  $\beta$  of the KWW equation. Overall, the time-dependence of molecular mobility during structural relaxation cannot be assessed from time-independent parameters alone. However, it is possible to investigate the parameters controlling molecular mobility at the beginning of an annealing experiment. The particular magnitude of such parameters may have an important effect on the evolution of the relaxation process that follows. It is also worthwhile to examine the contributions of individual parameters on the dynamics of materials exhibiting same nominal relaxation behavior, i.e., the same KWW relaxation function. Under this condition, materials would be regarded as having the same relaxation times through fitting to the KWW equation. However, it is still possible for these glasses to follow very different evolution paths in their molecular mobility during annealing.

The analysis presented in the previous section reveals that changes in molecular mobility over time, depend on four separate parameters: fragility ( $m$ ), glass transition temperature ( $T_g$ ), heat capacity change at  $T_g$  ( $\Delta C_{p,T_g}$ ), and the  $\gamma$  term related to the heat capacity of crystalline form. Even though many fragile materials are shown to have greater values of  $\Delta C_{p,T_g}$ , there are some exceptions, particularly with hydrogen bonded liquids, and no mathematical relationship has been established between  $m$  and  $\Delta C_{p,T_g}$ , i.e., between dynamic and thermodynamic fragility. The fact is that all four parameters are needed in order to construct a complete diagram depicting the evolution of the fictive temperature. In other words, to fully capture the time evolution of relaxation time during annealing.

## Fragility

The fragility is used to describe the non-Arrhenius temperature dependence of the structural relaxation time and is best quantified using the “fragility parameter”  $m$  as the effective activation enthalpy scaled by the available thermal energy at  $T_g$  (32). From the analysis presented in the preceding sections, it is possible to state that the fragility of glasses affects their physical stability in two ways: a) through its effect on the magnitude of the *initial* relaxation time, and b) through its effect on the *change* in relaxation time as the relaxation progresses.

a) Initial relaxation time. The terms  $B$  and  $T_0$  in our working equation Eq. (8) are both fragility related. The impact of fragility on molecular mobility can therefore be assessed by expressing  $B$  and  $T_0$  in terms of the fragility parameter,  $m$  [Eqs. (15) and (16)]. The relationship between the initial relaxation time of the (fresh) glass,  $\tau_{\text{glass}}^0$ , and the fragility,  $m$ , can be obtained by substituting Eqs. (15) and (16) into Eq. (21), after some rearrangement, we get:

$$\tau_{\text{glass}}^0 = \tau_0 \exp \left( \frac{(\ln 10)m_{\text{min}}^2}{(T/T_g) [m(1 - (T_g/T)^{1-\gamma}) + m_{\text{min}}(T_g/T)^{1-\gamma}]} \right) \quad (26)$$

Despite its rather knotty appearance, the above expression has important practical implications. It could help explain why two compounds with similar  $T_g$  could also exhibit completely different crystallization tendencies. Since  $T_g > T$ , Eq. (26) indicates that greater fragility results in longer initial relaxation times for the fresh glass. This effect is illustrated in Fig. 6, where the estimated initial relaxation times of two pharmaceutical compounds with very similar  $T_g$  (nifedipine,  $T_g = 320$  K and ritonavir,  $T_g = 323$  K) are shown as a function of temperature. The figure shows that the initial relaxation times for these two compounds diverge substantially as the temperature moves away from  $T_g$ . In fact, the two drugs are classified as fragile glasses [ $m_{\text{nifedipine}} = 57$  (33) and  $m_{\text{ritonavir}} = 107.3$  (34)]. Therefore, differences in fragility can be expected to contribute significantly to the resulting molecular mobility, and must be taken into consideration for the stability evaluation of the amorphous pharmaceuticals.

b) Change in relaxation time. Substituting Eqs. (15) and (16) into Eq. (8) gives:

$$\tau = \tau_0 \exp \left( \frac{(\ln 10)m_{\text{min}}^2 T_g}{(T/T_g) [m_{\text{min}} T_g - m(T_g - T_f)]} \right) \quad (27)$$

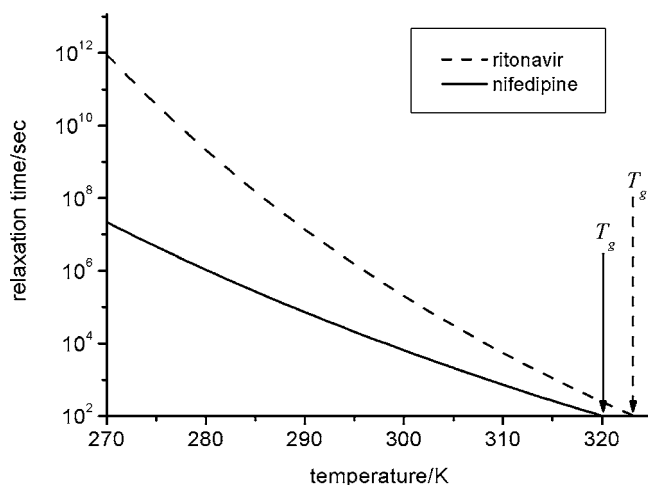


**Fig. 6.** Estimated initial relaxation times of two compounds with similar  $T_g$  but different relaxation behavior, nifedipine and ritonavir Eq. (26). The relaxation time at  $T_g$  was assumed to be 100 s. A  $\gamma$  value of 0.75 was used for both substances.



The above expression shows that with everything else equal, the more fragile material will experience a more rapid increase in  $\tau$ . From a practical perspective, however, it may be more relevant to consider the case where materials do not necessarily exhibit the exact same time dependence of  $T_f$ . If the more fragile material undergoes faster relaxation, the effect will be compounded, i.e., the increase in  $\tau$  with time will be even faster. Conversely, if the less fragile material undergoes faster relaxation, then the effect will be counteracted, slowing the change of  $\tau$  with time.

### Glass Transition Temperature

The glass transition temperature is the most widely used indicator for the physical stability of amorphous pharmaceuticals. Compounds with high  $T_g$  are more desirable candidates for development because the farther the storage temperature is from  $T_g$ , the lower the apparent molecular mobility materials exhibit.  $T_g$  alone is often employed as the qualitative approach to characterizing molecular motions. Storage temperature of at least 50 K below  $T_g$  is often recommended, since under such conditions, molecular motions could be considered negligible over the lifetime of the typical pharmaceutical products (4,12). An estimated relaxation time of 3–5 years is generally regarded as an ideal condition for the stability of amorphous formulations. However, it is important to notice that such a relaxation time corresponds to the average value over the entire duration of the experiment. Since changes in molecular mobility over time can be quite significant, it would be worthwhile to correlate the initial molecular mobility with the occurrence of destabilization events. The higher degree of molecular motion during the early storage stages, could lead to a situation where destabilization events such as crystal nucleation or appreciable chemical degradation take place even if the *time-average* molecular mobility is estimated to be sufficiently long.

The effect of  $T_g$  on the initial molecular mobility can be assessed by rearranging Eq. (26) as follows:

$$\tau_{glass}^0 = \tau_0 \exp \left( \frac{(\ln 10)m_{min}^2}{(mT/T_g) \left[ 1 - (T_g/T)^{1-\gamma} (1 - m_{min}/m) \right]} \right) \quad (28)$$

The above expression shows that reducing the storage temperature,  $T$ , leads to a quick increase of the,  $\tau_{glass}^0$ . Figure 7 shows the graphic form of Eq. (28), covering fragility values ( $m$ ) of ordinary amorphous organic pharmaceutical compounds. The figure points toward the set of conditions where the general rule-of-thumb of storing the amorphous material at  $T_g - T = 50$  K may not work. For compounds with high  $T_g$  but low fragility, it is possible to run into a situation where 50 K below  $T_g$  is not a sufficiently low temperature to ensure the physical stability of the product. The horizontal line in Fig. 7 marks a relaxation time of  $2 \times 10^4$  h ( $\sim 2.5$  year), which would make a reasonable pharmaceutical shelf life. The figure clearly shows that in some cases, the initial relaxation time can be substantially shorter than the desired value even if the material is stored 50 K below their  $T_g$ . For materials with  $m \approx 50$ , the initial relaxation time is too

short regardless of the  $T_g$ . Figure 7 also shows that 50 K below  $T_g$  is a suitable storage temperature for materials with  $m \approx 80$  as long as the  $T_g$  is not very high. Consequently, some caution should be exercised when the general rule of  $T_g - 50$  K is used, particularly for amorphous materials with high value of  $T_g$  (greater than  $\sim 350$  K) and low value of fragility (lower than  $\sim 80$ ).

### $\gamma$ Parameter

The  $\gamma$  parameter in the preceding equations is a measure of the loss of configurational enthalpy and entropy associated with the cooling of the glass. The smaller the  $\gamma$  term, the greater the loss of configurational entropy and enthalpy upon cooling of the glass. One immediate result of a  $\gamma$  value smaller than unity is the deviation from the Arrhenius temperature-dependence of the initial molecular mobility for freshly quenched glasses. In some instances,  $\tau_{glass}^0$  was estimated based on the assumption of  $\gamma = 1$  (11,28), resulting in a temperature-independent  $T_f$  equal to  $T_g$ . However, experimental results show that the value of  $\gamma$  can be considerably smaller than unity (see Table I). In such cases,  $T_g$  is an overestimate of the true fictive temperature, particularly when the storage temperature is far away from  $T_g$ . For example, the initial fictive temperature of sorbitol stored at  $T_g - 25$  K was found to be 10 K lower than  $T_g$ . Differences of such magnitude can translate into significant differences in initial molecular mobility and in its time-dependence during relaxation, as seen in Fig. 8. In this figure, estimated relaxation times for sorbitol, without considering the  $\gamma$  parameter (i.e., with  $\gamma = 1$ ), result in overestimates of molecular mobility of over one order of magnitude. These results affirm the importance of evaluating  $\gamma$  for molecular mobility determinations, despite the added (but manageable) experimental complications involved by the  $C_p$  measurements of the crystalline form.

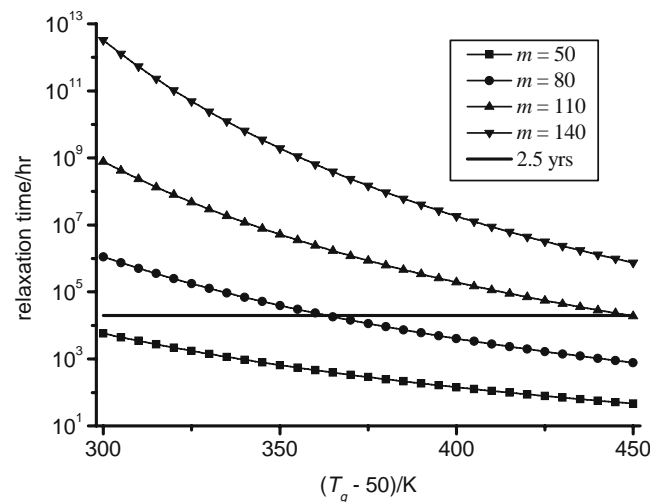


**Fig. 7.** Estimated initial relaxation times versus  $T_g$  of amorphous compounds with different fragility, stored at temperature 50 K below  $T_g$  Eq. (28). A  $\gamma$  value of 0.75 was used in the calculations.

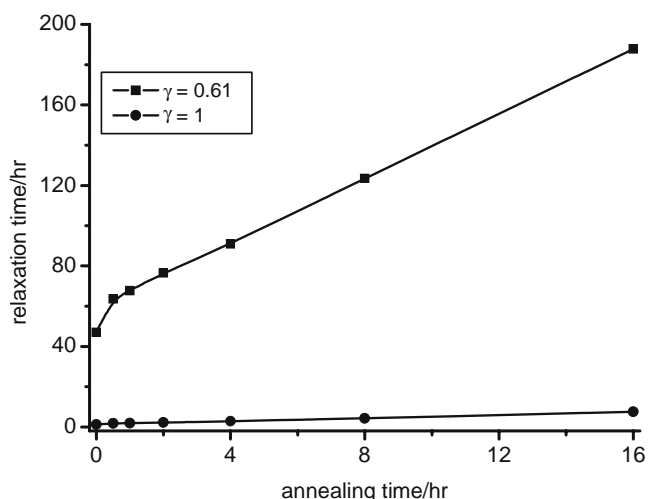


**Fig. 8.** Comparison of the evolution of estimated relaxation times of sorbitol annealed at temperature 25 K below  $T_g$  with and without the consideration of heat capacity difference between the glass and crystalline forms.

### Applicability of the KWW Equation for Molecular Mobility Evaluation

At present, the molecular mobility of amorphous pharmaceutical solids is primarily evaluated by fitting the KWW equation to data obtained from DSC-based enthalpy recovery experiments. This method gives a fitted average enthalpy relaxation time ( $\tau_{\text{KWW}}$ ) and the corresponding stretch parameter  $\beta$ . The popularity of this purely empirical approach is arguably due to its experimental simplicity. For the very same reasons, however, besides the numerical values for the two fitted parameters, the KWW model provides no fundamental information regarding the mobility attributes of amorphous substances. In essence,  $\tau_{\text{KWW}}$  should be regarded as an approximated measure of molecular mobility averaged

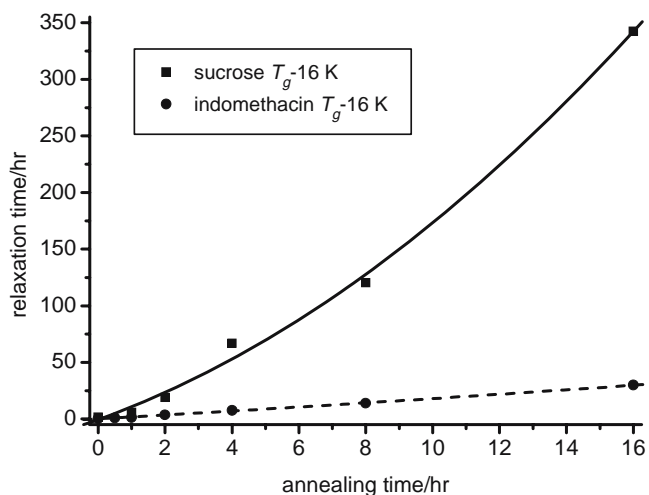


**Fig. 9.** The estimated time-dependence of relaxation times for amorphous sucrose and indomethacin, both stored at temperature 16 K below  $T_g$ . The relaxation times estimated from KWW equation were very close (sucrose:  $\tau_{\text{KWW}} = 4.2$  h,  $\beta = 0.59$ ; indomethacin:  $\tau_{\text{KWW}} = 3.9$  h,  $\beta = 0.62$ ).

over the entire duration of the enthalpy recovery experiment. Consequently, to the extent that  $\tau$  varies with time during annealing, the KWW approach is not an appropriate descriptor of the relaxation process. Considering that in our annealing experiments we have observed changes in  $\tau$  of one order of magnitude or more, and that changes of two orders of magnitude have been anticipated (6), we can say that the use of the KWW approach is severely limited at best.

The limitations of the KWW approach are illustrated in Fig. 9, where the time-dependence of relaxation times were compared between amorphous indomethacin and amorphous sucrose, both stored at a temperature 16 K below  $T_g$ . The evolution of the relaxation time for each material is quite different as seen in the figure. However, their  $\tau_{\text{KWW}}$  and  $\beta$  values, obtained from the enthalpy recovery data are very close to each other (sucrose:  $\tau_{\text{KWW}} = 4.2$  hr,  $\beta = 0.59$ ; indomethacin:  $\tau_{\text{KWW}} = 3.9$  hr,  $\beta = 0.62$ ). It has been reported that amorphous indomethacin, when stored around  $T_g - 16$  K could easily transform to crystalline forms in less than 100 days (2), whereas no crystallization takes place for sucrose under the same conditions. The different crystallization tendency between these two materials correlates very well with the estimated time-dependence of their relaxation times. Such important information, however, is completely lost with the application of the KWW model, which leads in fact to the conclusion of very similar molecular mobility for the two materials. It is important to clarify at this point that molecular mobility is not the only factor determining the crystallization tendency of amorphous materials. Other important factors, such as the thermodynamic driving force for example (difference in free energy between the amorphous and crystalline forms), are also at play. But molecular mobility is always an important factor.

### Limitations of KWW Approach for Practical Purposes

There is a great deal of interest in preparing amorphous solid dispersions of drugs with additives, in order to improve the physical and chemical stability of these pharmaceutical

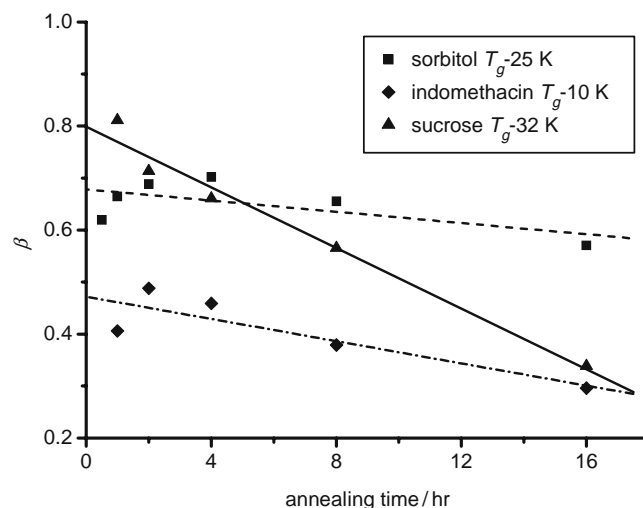


**Fig. 10.** The  $\beta$  values solved from the KWW equation using the time-dependent  $\tau$  data.

systems (35–38). One of the most widely used means to assess the stabilization effects of different solid dispersions is to compare their  $\tau_{\text{KWW}}$  (36,39,40). However, the results from such comparison may be questionable because the fitted  $\beta$  values of these systems may vary substantially. Considering that  $\beta$  is merely a curve-fitting parameter, and that the distribution of relaxation time will have profound effect on the molecular mobility of amorphous systems, Shamblin and Hancock (7) indicated that  $\tau_{\text{KWW}}$  can only be compared when the values of  $\beta$  differ by less than 0.1. This restriction greatly reduces the applicability of the KWW approach as a suitable way of making comparisons of molecular mobility. In light of the limitations resulting from the KWW approach, the method developed in this article can serve as an alternative approach for the estimation of molecular mobility. The approach presented here is based on two models, one theoretical (Adam-Gibbs) and one empirical (VTF). However, unlike the KWW model, the approach proposed here (Eqs. 8, 19, 21 and 24) exclusively contains parameters that are a) physically meaningful, and consequently, b) experimentally and independently accessible, i.e., measurable. This approach allows us to estimate the time-dependence of molecular mobility, adding a much needed alternative to the study of the molecular motions in amorphous solids. It is our belief that the proposed methodology can help provide more and better clues toward a fundamental understanding of the underlying correlation between the molecular mobility and the stability of amorphous pharmaceutical systems.

### Changes in $\beta$

Since the enthalpy recovery data are required for the estimation of time-dependent  $\tau$ , the evolution of  $\beta$  with time during relaxation can also be assessed by solving the KWW equation for  $\beta$ . Examples of the changes in  $\beta$  for our model compounds are shown in Fig. 10. In most systems,  $\beta$  decreases with time, suggesting increasing non-exponential behavior as systems continue to relax toward the equilibrium supercooled liquid. This result agrees with the general observation for structural relaxation behavior (6). If  $\beta$  is assumed to reflect the breadth of the distribution times, one can then conclude that continued relaxation will lead to a broader distribution of relaxation times. A similar conclusion was reached by Shamblin *et al.* from their simulation work (29). The obtained results show that in some instances, the solved  $\beta$  value falls outside the interval [0, 1], making impossible any physical interpretation of the  $\beta$  parameter. From the foregoing discussion, this situation should not be surprising. Because of its empirically based, parameter fitting nature, the KWW equation can fail to provide accurate descriptions of the relaxation behavior, particularly in the short-time regime (41).

### CONCLUSIONS

The time-dependence of molecular mobility can be estimated from the nonlinear Adam-Gibbs equation coupled with fragility and fictive temperature measurements using DSC. Our investigation on the evolution of relaxation enthalpy for amorphous pharmaceutical compounds stored

at temperatures below their  $T_g$  revealed that increases in  $\tau$  by several orders of magnitude are possible within the timescale of the experiment. The decrease of molecular motions over time, which could sometimes be dramatic, is evident among amorphous pharmaceutical solids under isothermal conditions. Such significant changes must be taken into consideration when the timescale of the molecular motions are evaluated to assess stability of amorphous drugs. The results show that the time-dependent  $\tau$  values obtained using this approach offer a significant improvement over estimations based on the KWW equation, which rely on a single averaged  $\tau$  value for relating molecular mobility to the crystallization tendencies of amorphous drug substances. The analysis presented here helps provide a quantitative explanation as to why two materials with very similar glass transition temperature can exhibit very different crystallization tendencies. Moreover, the same analysis can quantitatively explain why two materials exhibiting similar degrees of KWW-estimated molecular mobility, could also exhibit very different crystallization tendencies. Our findings indicate that molecular mobility is in fact, and should be viewed as, a dynamic process with a strong potential to quickly change, even under isothermal conditions. This view of the molecular mobility should prove useful in efforts aimed at the fundamental understanding of the stability of amorphous pharmaceutical systems as well as in efforts to improve their shelf life.

### ACKNOWLEDGMENT

This study is financially supported by The Purdue-Michigan Program on the Chemical and Physical Stability of Pharmaceutical Solids.

### REFERENCES

1. Y. Aso, S. Yoshioka, and S. Kojima. Molecular mobility-based estimation of the crystallization rates of amorphous nifedipine and phenobarbital in poly(vinylpyrrolidone) solid dispersions. *J. Pharm. Sci.* **93**:384–391 (2004).
2. V. Andronis, M. Yoshioka, and G. Zografis. Effects of sorbed water on the crystallization of indomethacin from the amorphous state. *J. Pharm. Sci.* **86**:346–351 (1997).
3. Y. S. Guo, S. R. Bryn, and G. Zografis. Physical characteristics and chemical degradation of amorphous quinapril hydrochloride. *J. Pharm. Sci.* **89**:128–143 (2000).
4. S. R. Byrn, W. Xu, and A. W. Newman. Chemical reactivity in solid-state pharmaceuticals: formulation implications. *Adv. Drug Deliv. Rev.* **48**:115–136 (2001).
5. M. J. Pikal and S. Shah. The collapse temperature in freeze-drying—dependence on measurement methodology and rate of water removal from the glassy phase. *J. Phys. Chem.* **62**:165–186 (1990).
6. K. Kawakami and M. J. Pikal. Calorimetric investigation of the structural relaxation of amorphous materials: evaluating validity of the methodologies. *J. Pharm. Sci.* **94**:948–965 (2005).
7. B. C. Hancock and S. L. Shamblin. Molecular mobility of amorphous pharmaceuticals determined using differential scanning calorimetry. *Thermochim. Acta* **380**:95–107 (2001).
8. J. S. Liu, D. R. Rigsbee, C. Stotz, and M. J. Pikal. Dynamics of pharmaceutical amorphous solids: the study of enthalpy relaxation by isothermal microcalorimetry. *J. Pharm. Sci.* **91**:1853–1862 (2002).

9. K. Kawakami and Y. Ida. Direct observation of the enthalpy relaxation and the recovery processes of maltose-based amorphous formulation by isothermal microcalorimetry. *Pharm. Res.* **20**:1430–1436 (2003).
10. S. P. Duddu, G. Z. Zhang, and P. R. DalMonte. The relationship between protein aggregation and molecular mobility below the glass transition temperature of lyophilized formulations containing a monoclonal antibody. *Pharm. Res.* **14**:596–600 (1997).
11. V. Andronis and G. Zografi. The molecular mobility of supercooled amorphous indomethacin as a function of temperature and relative humidity. *Pharm. Res.* **15**:835–842 (1998).
12. B. C. Hancock, S. L. Shamblin, and G. Zografi. Molecular mobility of amorphous pharmaceutical solids below their glass-transition temperatures. *Pharm. Res.* **12**:799–806 (1995).
13. V. Andronis and G. Zografi. Molecular mobility of supercooled amorphous indomethacin, determined by dynamic mechanical analysis. *Pharm. Res.* **14**:410–414 (1997).
14. S. Yoshioka, Y. Aso, S. Kojima, S. Sakurai, T. Fujiwara, and H. Akutsu. Molecular mobility of protein in lyophilized formulations linked to the molecular mobility of polymer excipients, as determined by high resolution C-13 solid-state NMR. *Pharm. Res.* **16**:1621–1625 (1999).
15. S. Yoshioka, Y. Aso, and S. Kojima. Determination of molecular mobility of lyophilized bovine serum albumin and gamma-globulin by solid-state H-1 NMR and relation to aggregation-susceptibility. *Pharm. Res.* **13**:926–930 (1996).
16. S. L. Shamblin, B. C. Hancock, Y. Dupuis, and M. J. Pikal. Interpretation of relaxation time constants for amorphous pharmaceutical systems. *J. Pharm. Sci.* **89**:417–427 (2000).
17. G. Adam and J. H. Gibbs. On temperature dependence of cooperative relaxation properties in glass-forming liquids. *J. Chem. Phys.* **43**:139–146 (1965).
18. A. Q. Tool and C. G. Eichlin. Variations caused in the heating curves of glass by heat treatment. *J. Am. Ceram. Soc.* **14**:276–308 (1931).
19. I. M. Hodge. Enthalpy relaxation and recovery in amorphous materials. *J. Non-Cryst. Solids* **169**:211–266 (1994).
20. G. W. Scherer. Use of the Adam-Gibbs equation in the analysis of structural relaxation. *J. Am. Ceram. Soc.* **67**:504–511 (1984).
21. D. J. Plazek and J. H. Magill. Physical properties of aromatic hydrocarbons. I. Viscoelastic behavior of 1,3,5-tri-alpha-naphthyl benzene. *J. Chem. Phys.* **45**:3038–3050 (1966).
22. M. A. Debolt, A. J. Easteal, P. B. Macedo, and C. T. Moynihan. Analysis of structural relaxation in glass using rate heating data. *J. Am. Ceram. Soc.* **59**:16–21 (1976).
23. C. T. Moynihan, A. J. Easteal, J. Wilder, and J. Tucker. Dependence of glass-transition temperature on heating and cooling rate. *J. Phys. Chem.* **78**:2673–2677 (1974).
24. B. C. Hancock, C. R. Dalton, M. J. Pikal, and S. L. Shamblin. A pragmatic test of a simple calorimetric method for determining the fragility of some amorphous pharmaceutical materials. *Pharm. Res.* **15**:762–767 (1998).
25. R. Bohmer and C. A. Angell. Correlations of the nonexponentiality and state dependence of mechanical relaxations with bond connectivity in Ge-as-Se supercooled liquids. *Phys. Rev. B* **45**:10091–10094 (1992).
26. R. Bohmer, K. L. Ngai, C. A. Angell, and D. J. Plazek. Nonexponential relaxations in strong and fragile glass formers. *J. Chem. Phys.* **99**:4201–4209 (1993).
27. B. C. Hancock and G. Zografi. Characteristics and significance of the amorphous state in pharmaceutical systems. *J. Pharm. Sci.* **86**:1–12 (1997).
28. K. J. Crowley and G. Zografi. The use of thermal methods for predicting glass-former fragility. *Thermochim. Acta* **380**:79–93 (2001).
29. S. L. Shamblin, X. L. Tang, L. Q. Chang, B. C. Hancock, and M. J. Pikal. Characterization of the time scales of molecular motion in pharmaceutically important glasses. *J. Phys. Chem. B* **103**:4113–4121 (1999).
30. S. L. Shamblin and G. Zografi. Enthalpy relaxation in binary amorphous mixtures containing sucrose. *Pharm. Res.* **15**:1828–1834 (1998).
31. M. Goldstein. Viscous-liquids and glass-transition. 5. Sources of excess specific-heat of liquid. *J. Chem. Phys.* **64**:4767–4774 (1976).
32. I. M. Hodge. Strong and fragile liquids—a brief critique. *J. Non-Cryst. Solids* **202**:164–172 (1996).
33. Y. Aso, S. Yoshioka, and S. Kojima. Explanation of the crystallization rate of amorphous nifedipine and phenobarbital from their molecular mobility as measured by C-13 nuclear magnetic resonance relaxation time and the relaxation time obtained from the heating rate dependence of the glass transition temperature. *J. Pharm. Sci.* **90**:798–806 (2001).
34. D. L. Zhou, G. G. Z. Zhang, D. Law, D. J. W. Grant, and E. A. Schmitt. Physical stability of amorphous pharmaceuticals: importance of configurational thermodynamic quantities and molecular mobility. *J. Pharm. Sci.* **91**:1863–1872 (2002).
35. J. J. Li, Y. S. Guo, and G. Zografi. The solid-state stability of amorphous quinapril in the presence of beta-cyclodextrins. *J. Pharm. Sci.* **91**:229–243 (2002).
36. T. Matsumoto and G. Zografi. Physical properties of solid molecular dispersions of indomethacin with poly(vinylpyrrolidone) and poly(vinylpyrrolidone-co-vinylacetate) in relation to indomethacin crystallization. *Pharm. Res.* **16**:1722–1728 (1999).
37. X. M. Zeng, G. P. Martin, and C. Marriott. Effects of molecular weight of polyvinylpyrrolidone on the glass transition and crystallization of co-lyophilized sucrose. *Int. J. Pharm.* **218**:63–73 (2001).
38. Y. Hu. Solid-state investigation of crystalline and amorphous lisinopril and stabilization of amorphous lisinopril and quinapril hydrochloride. *Industrial and Physical Pharmacy*, Ph. D., Purdue University, West Lafayette, 2001.
39. L. R. Hilden and K. R. Morris. Prediction of the relaxation behavior of amorphous pharmaceutical compounds. I. Master curves concept and practice. *J. Pharm. Sci.* **92**:1464–1472 (2003).
40. V. K. Kakumanu and A. K. Bansal. Enthalpy relaxation studies of celecoxib amorphous mixtures. *Pharm. Res.* **19**:1873–1878 (2002).
41. G. Williams. Molecular-motion in glass-forming systems. *J. Non-Cryst. Solids* **131**:1–12 (1991).
42. R. Surana, A. Pyne, and R. Suryanarayanan. Effect of preparation method on physical properties of amorphous trehalose. *Pharm. Res.* **21**:1167–1176 (2004).